

Stereochemical Dependence of the Self-Assembly of the Immunoadjuvants Pam₃Cys and Pam₃Cys-Ser

Frank Reichel,[†] Annie M. Roelofsen,[‡] Hubertus P. M. Geurts,[§] Taina I. Hämäläinen,[†] Martinus C. Feiters,[‡] and Geert-Jan Boons^{*,†}

Contribution from the School of Chemistry, The University of Birmingham, Edgbaston, Birmingham, B15 2TT, United Kingdom, Department of Organic Chemistry, NSR Institute for Molecular Structure, Design and Synthesis, University of Nijmegen, Toernooiveld, NL 6525 ED Nijmegen, The Netherlands, and Department of Organic Chemistry, Central Microscopy Facility, University of Nijmegen, Toernooiveld, NL 6525 ED Nijmegen, The Netherlands

Received April 23, 1999

Abstract: The lipopeptide tripalmitoyl-*S*-glycerylcysteine (Pam₃Cys) is derived from the *N*-terminal part of bacterial lipopeptides and is a polyclonal B-lymphocyte and macrophage activator. Derivatives of Pam₃Cys constitute highly potent, nontoxic immunoadjuvants, and lipopeptide–antigen conjugates have found important applications as novel fully synthetic low-molecular-weight vaccines. To establish a possible correlation between molecular structure, aggregation properties, and biological activities, we have studied the self-assembly and monolayer properties of a range of Pam₃Cys derivatives using transmission electron microscopy (TEM) and a Langmuir–film balance combined with a Brewster angle microscopy (BAM). It was found that the chirality of the glyceryl moiety and the additional serine unit impacted on the mode of aggregation and the monolayer properties. Correlations are discussed between these physicochemical properties and biological activities.

Introduction

Lipoproteins found in the outer membrane of *Escherichia coli* are potent activators of B-lymphocytes and macrophages.¹ The *N*-terminus of the protein part is linked to a *S*-(dihydroxypropyl)-cysteine moiety, which, in turn, is linked to a mixture of three fatty acids, palmitic acid being the main one. The synthetic derivative, tri-palmitoyl-*S*-glycerylcysteine (Pam₃Cys), has been determined as the smallest biologically active compound.² Antigen-specific antibodies can be elicited with low-molecular-weight conjugates of Pam₃Cys with peptide- or saccharide-based haptens.³ Such constructs are successfully used as fully synthetic

vaccines. For example, a recently developed low-molecular-weight synthetic vaccine against foot-and-mouth disease contains a helical peptide as a hapten and Pam₃Cys as an in-built adjuvant.⁴ A similar fully synthetic experimental AIDS vaccine composed of a multi antigen peptide system, a peptide antigen, and Pam₃Cys has been described.⁵ Recently, we reported⁶ the synthesis of a saccharide–peptide–lipopeptide conjugate, which is under investigation as a potential vaccine against *Neisseria meningitidis*. These examples highlight that lipopeptide–antigen conjugates represent a promising alternative to conventional and recombinant protein vaccines.

The desirable immunological properties of Pam₃Cys conjugates probably arise from their intrinsic adjuvant properties, such as B-cell and macrophage activators and their ability to self-assemble into macromolecular aggregates. In general, small molecules are unable to stimulate a sustainable antibody response. However, a much-improved immunological reaction is observed when small haptens are coupled at the surface of macromolecules. Traditionally, antigenic macromolecules were obtained by conjugation of a hapten to a carrier protein; however, it is now recognized that self-assembled aggregates can also function as efficient immunogens.

Jung and co-workers⁸ have investigated in great detail the molecular requirements of Pam₃Cys derivatives for optimal immunological activities and found that (i) the lipopeptide Pam₃Cys-Ser, which has an additional polar serine moiety, is

* To whom correspondence should be addressed. Present address: Complex Carbohydrate Research Center, University of Georgia, 220 Riverbend Road, Athens, Georgia 30602-4712. Tel: 706-642-4401. Fax: 706-542 4412. E-mail: gjboons@ccrc.uga.edu.

[†] The University of Birmingham.

[‡] NSR Institute for Molecular Structure, Design and Synthesis, University of Nijmegen.

[§] Central Microscopy Facility, University of Nijmegen.

(1) (a) Braun, V.; Rehn, K. *Eur. J. Biochem.* **1969**, *1*, 426. (b) Braun, V. *Biochim. Biophys. Acta* **1975**, *415*, 335.

(2) (a) Bessler, W. G.; Cox, M.; Lex, A.; Suhr, B.; Weismüller, K.-H.; Jung, G. *J. Immunol.* **1985**, *135*, 1900–1905. (b) Hoffmann, P.; Wiesmüller, K.-H.; Metzger, J.; Jung, G.; Bessler, W. G. *Biol. Chem. Hoppe-Seyler* **1989**, *370*, 6, 575–582. (c) Seifert, R.; Serke, S.; Huhn, D.; Bessler, W. G.; Hauschildt, S. *Biochem. J.* **1990**, *267*, 3, 795–802. (d) Wiedemann, F.; Link, R.; Pumpe, K.; Jacobshagen, U.; Schaefer, H. E.; Wiesmüller, K.-H.; Hummel, R.-P.; Jung, G.; Bessler, W.; Boltz, T. *J. Pathol.* **1991**, *164*, 3, 265–271.

(3) (a) Jung, G.; Wiesmüller, K.-H.; Becker, G.; Bühring, H. J.; Bessler, W. G. *Angew. Chem., Int. Ed. Engl.* **1985**, *24*, 10, 872–873. (b) Deres, K.; Schild, H.; Wiesmüller, K. H.; Jung, G.; Rammensee, H. G. *Nature* **1989**, *342*, 6249, 561–564. (c) Reitermann, A.; Metzger, J.; Wiesmüller, K.-H.; Jung, G.; Bessler, W. G. *Biol. Chem. Hoppe-Seyler* **1989**, *370*, 4, 343–352. (d) Metzger, J. W.; Wiesmüller, K. H.; Jung, G. *Int. J. Pept. Protein Res.* **1991**, *38*, 545. (e) Wiesmüller, K. H.; Bessler, W. G.; Jung, G. *Int. J. Pept. Protein Res.* **1992**, *40*, 3–4, 255–260. (f) DeOgny, L.; Pramanik, B. C.; Arndt, L. L.; Jones, J. D.; Rush, J.; Slaughter, C. A.; Radolf, J. D.; Norgard, M. V. *Pept. Res.* **1994**, *7*, 2, 91–97.

(4) Weismüller, K.-H.; Jung, G.; Hess, G. *Vaccine* **1989**, *7*, 1, 29–33. (5) Defoort, J.-P.; Nardelli, B.; Huang, W.; Ho, D. D.; Tam, J. P. *Proc. Natl. Acad. Sci. U.S.A.* **1992**, *89*, 9, 3879–3883.

(6) Reichel, F.; Ashton, P. R.; Boons, G. J. *Chem. Commun.* **1997**, *21*, 2087–2088.

(7) (a) Lerner, R. A. *Nature (London)* **1988**, *299*, 592–596. (b) Dimarchi, R.; Brooke, G.; Gale, C.; Cracknell, V.; Doel, T.; Mowat, N. *Science* **1986**, *232*, 4750, 639–641.

(8) Metzger, J.; Jung, G.; Bessler, W. G.; Hoffmann, P.; Strecker, M.; Lieberknecht, A.; Schmidt, U. *J. Med. Chem.* **1991**, *34*, 7, 1969–1974.

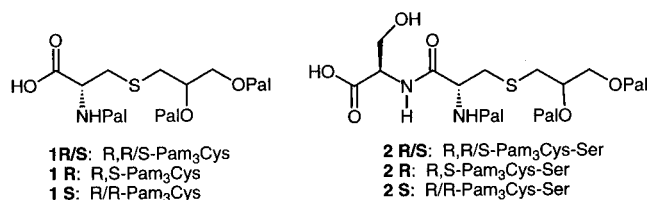


Figure 1. Pam₃Cys and Pam₃Cys-Ser derivatives.

much more mitogenic than Pam₃Cys and is the preferred compound for use in vaccines. (ii) The peptide sequence can be varied (length, sequence) without loss of biological activity. (iii) The length of the fatty acid chains has only a marginal influence, but three acyl chains give an optimum biological activity. (iv) Lipopeptides with *R*-configuration in the glycerol moiety have a higher activity than the corresponding *S*-diastereoisomers.

As part of a program to investigate a possible correlation between molecular structures, aggregation properties, and biological activities of Pam₃Cys derivatives, we have studied the self-assembly and monolayer properties of the compounds **1** and **2** using transmission electron microscopy (TEM) and a Langmuir-film balance combined with a Brewster angle microscopy (BAM).

Results and Discussion

Electron Microscopy Studies. Diastereoisomeric mixtures of Pam₃Cys (**1S/R**) and Pam₃Cys-Ser (**2S/R**), as well as optically pure compounds **1R**, **1S**, **2R**, and **2S** (Figure 1), were prepared according to literature or modified literature methodologies.^{3d,9}

Water suspensions of the compounds, prepared by a modified ethanol injection method, were studied by transmission electron microscopy (TEM). The results of the study are summarized in Table 1. The diastereoisomeric mixture of Pam₃Cys (**1R/S**) formed vesicles with an average diameter of approximately 210 nm but which could be as large as 640 nm as seen by Pt-shadowing (not shown) and negative staining (Figure 2a). Freeze fracturing experiments showed that the vesicles were composed of multilamellar bilayers (Figure 2b). The observed morphology did not change upon aging. The pure diastereoisomers **1R** and **1S** displayed different self-assembly properties. Initially, **1R** and **1S** formed relatively small vesicles with diameters in the range of 50–105 and 20–230 nm, respectively (not shown). After an aging period of 5 days, the vesicles reorganized to mainly tubular or rodlike structures which reached a length of approximately 2 μm for **1R** (Figure 2c) and **1S**. Interestingly, the intermediate structures shown in Figure 2d suggest that tube or rod formation proceeds by elongation and fusion of vesicular structures. Tubular and rodlike structures are considered to be more ordered than vesicles, and their formation has been explained by several theories. For example, it has been suggested that a common mode of tube formation is by rolling-up of bilayers.¹⁰ Some molecular structural features such as chirality¹¹ and diacetylenic lipids¹² are known to promote tubular aggregation, but the limited number of compounds

known to organize into these structures makes it difficult to predict this mode of assembly.

The coupling of an additional serine residue to Pam₃Cys leads to a compound that has significantly improved immunological properties, and it was found that this modification also affected its self-assembly behavior. Pt-shadowing experiments of a water suspension of Pam₃Cys-Ser (**2S/R**) displayed flat bilayers as the dominating structure, which was sometimes round shaped (Figure 3a). After aging for 7 days, extended structures, which reached a length of approximately 380 nm (Figure 3b), were observed. Some of these structures appeared to be flattened and had a width of 77 nm, which is twice the width of nonflattened structures. The negative staining experiment, where uranyl acetate was applied before the aggregate was exposed to vacuum, gave further indications of the presence of tubular structures (Figure 3c). On the other hand, the diastereoisomerically pure compounds **2S** and **2R** already exhibited nonflattened extended structures in freshly prepared aqueous suspensions (Figure 3d), which reached a length of up to 3 μm and a width of approximately 20–50 nm and formed a dense network in the aged sample (Figure 3e). Unfortunately, structures could not be visualized in freeze fracturing experiments of samples that contained low concentrations of material.

Thus, the optically pure compounds **2S** and **2R** form highly ordered extended aggregates¹⁰ without the need of aging, whereas the epimeric mixture **2S/R** initially formed vesicles which, upon aging, rearranged to extended structures. A possible explanation of this phenomenon is that the vesicles are composed of both diastereoisomers of **2**. Upon aging, however, a chiral separation takes place to give thermodynamically more stable extended aggregates that contain only one of the two epimers.

Monolayer Studies. It has been reported¹³ that diastereoisomeric mixtures of compounds **1S/R** form viscous monolayers. The main argument for this conclusion is based on the following observations. (i) Hysteresis experiments showed that the surface pressure of the compressed monolayer decreased during the waiting period, which was probably due to continuous compression of the monolayer when the barrier had stopped. In addition, the second compression was steeper and showed smaller compressibility at identical molecular areas, indicating that the molecules were more densely packed compared to the first compression. (ii) The isotherm showed a decrease in compressibility and a higher collapse pressure with temperature, which was in line with the expected decrease in viscosity with temperature. (iii) Compression at the so-called thermodynamic mode, where the monolayer is only compressed further when the monolayer has relaxed to equilibrium pressure, led to a smaller compressibility.¹⁴

We have extended the monolayer studies to the diastereoisomerically pure compounds **1S**, **1R**, **2S**, and **2R**. The molecular areas and collapse pressures as functions of compression rates and temperature have been measured, and hysteresis experiments have been performed. The deduced molecular areas at which the monolayers form solid analogous states on a water surface at 20 °C are summarized in Table 2.

(9) (a) Wiesmüller, K. H.; Bessler, W. G.; Jung, G. *Hoppe-Seyler's Z. Physiol. Chem.* **1983**, *364*, 5, 593–606. (b) Kurimura, M.; Takemoto, M.; Achiwa, K. *Chem. Pharm. Bull.* **1990**, *38*, 4, 1110–1112. (c) Kurimura, M.; Takemoto, M.; Achiwa, K. *Chem. Pharm. Bull.* **1991**, *39*, 10, 2590–2596.

(10) (a) Fuhrhop, J.-H.; Schnieder, P.; Boekema, E.; Helfrich, W. *J. Am. Chem. Soc.* **1988**, *110*, 9, 2861–2867. (b) Fuhrhop, J.-H.; Helfrich, W. *Chem. Rev.* **1993**, *93*, 4, 1565–1582 and references therein.

(11) (a) Fuhrhop, J.-H.; Schnieder, P.; Rosenberg, J.; Boekema, E. *J. Am. Chem. Soc.* **1987**, *109*, 11, 3887–3390. (b) Selinger, J. V.; MacKintosh, F. C.; Schnur, J. M. *Phys. Rev. E* **1996**, *53*, 4, 3804–3818, and references therein.

(12) (a) Georger, J. H.; Singh, A.; Price, R. R.; Schnur, J. M.; Yager, P.; Schoen, P. *J. Am. Chem. Soc.* **1987**, *109*, 20, 6169–6175. (b) Schnur, J. M.; Price, R.; Schoen, P.; Yager, P.; Calvert, J. M.; Georger, J.; Singh, A. *Thin Solid Films* **1987**, *152*, 1–2, 181–206. (c) Rhodes, D. G.; Blechner, S. L.; Yager, P.; Schoen, P. *Chem. Phys. Lipids* **1987**, *49*, 39. (d) Schnur, J. M. *Science* **1993**, *262*, 5140, 1669–1676. (e) Schnur, J. M.; Ratna, B. R.; Selinger, J. V.; Jyothi, G.; Easwaram, K. R. K. *Science* **1994**, *264*, 5161, 945–947.

(13) Prass, W.; Ringsdorf, H.; Bessler, W.; Wiesmüller, K. H.; Jung, G. *Biochim. Biophys. Acta* **1987**, *900*, 1, 116–128.

(14) Albrecht, O. *Thin Solid Films* **1983**, *99*, 1–3, 227–234.

Table 1. TEM Observations of Supra-Structures in Aqueous Media^a

	morphologies of fresh preparations	size	morphologies of aged preparations ^b	size
IR/S	vesicles	$d = 160\text{--}640$ nm	unchanged	
IR	vesicles	$d = 50\text{--}105$ nm NS: $d = 78\text{--}1400$ nm	vesicles tubes	$d = 50\text{--}105$ nm $L = 260\text{--}2500$ nm $W = \sim 25$ nm
IS	vesicles	$d = 20\text{--}230$ nm	vesicles tubes	$d = 60\text{--}230$ nm $L = 700\text{--}2300$ nm $W = 40\text{--}70$ nm
2R/S	layers vesicles tubes (few)	$d = 25\text{--}55$ nm $L = 230\text{--}360$ nm $W = 20\text{--}50$ nm	tubes (dominating)	$L = 230\text{--}1900$ nm $W = \sim 38$ nm (flat sections: $W = 77$ nm)
2R	fibers/tubes	$L = 154\text{--}3600$ nm $W = 25\text{--}40$ nm	layers network of fibers/tubes	$L = > 1500$ nm $W = \sim 30$ nm
2S	vesicles (few) fibers/tubes	$d = 40\text{--}70$ nm $L = 260\text{--}2000$ nm $W = 25\text{--}50$ nm	network of fibers/tubes	$L = > 1500$ nm $W = \sim 30$ nm
	vesicles (few) layers	$d = 25\text{--}50$ nm $d_{\text{roundlayers}} = \sim 60$ nm		

^a The experiments have been performed by Pt-shadowing and negative staining; L = length; W = width; d = diameter; NS = negative staining.
^b Aging after 5 or 7 days.

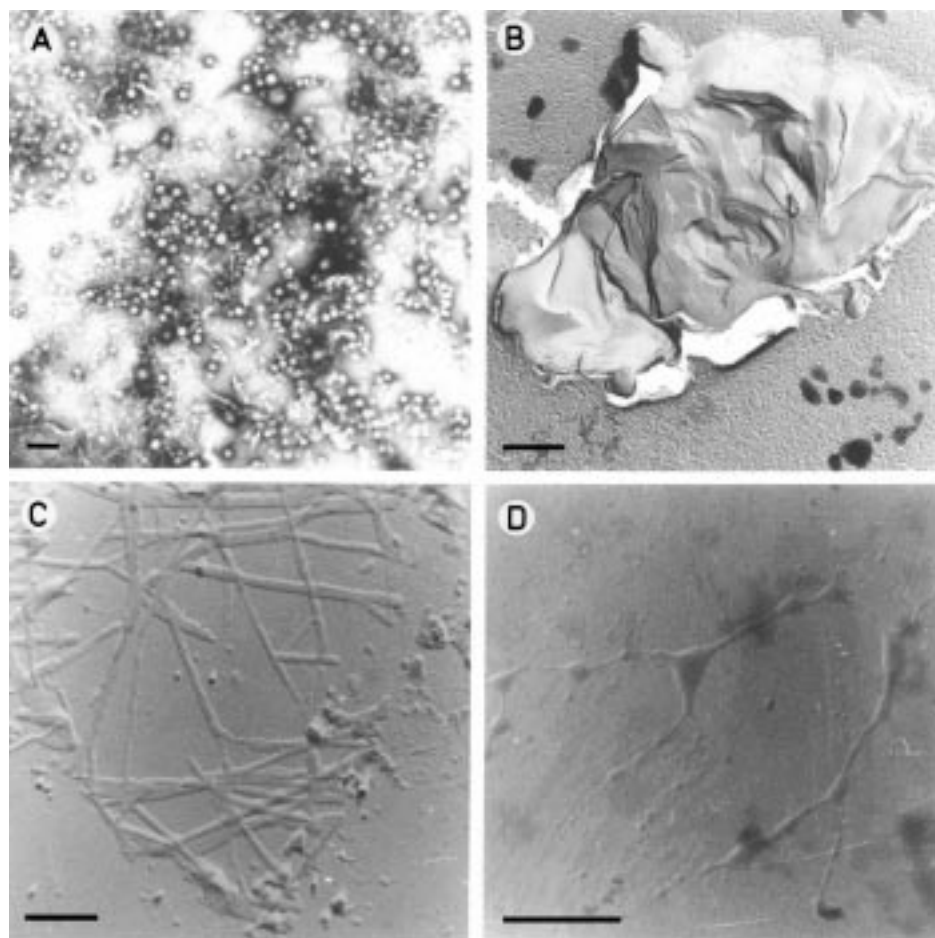


Figure 2. Electron micrographs of Pam₃Cys derivatives (**1**). Bar represents 500 nm. (A) Negative staining of **1R/S**; (B) freeze fracturing of **1R/S**; (C) Pt shadowing of **1R** after aging of 5 days; (D) Pt shadowing of **1S** after aging 5 days.

The compounds **2R/S**, **2R**, and **2S** showed very similar molecular areas and isotherms, and it is concluded that the stereochemistry of these compounds has no detectable impact on the monolayer properties.

As shown in Table 2, the diastereoisomeric mixture of Pam₃Cys (**1S/R**) can be compressed significantly more tightly than the diastereoisomerically pure compounds **1S** and **1R**. The values for the molecular areas, however, are typical of am-

phiphiles with three alkyl chains. The system used for the characterization of monolayers (Experimental Section) is different from the one used in the above-described experiments.¹³ The equipment used in this study is not computerized to allow true thermodynamic mode measurements. On the other hand, the system has two moving barriers and the difference in surface pressure between the barrier and the point of measurement is therefore smaller than in the case of compression with one

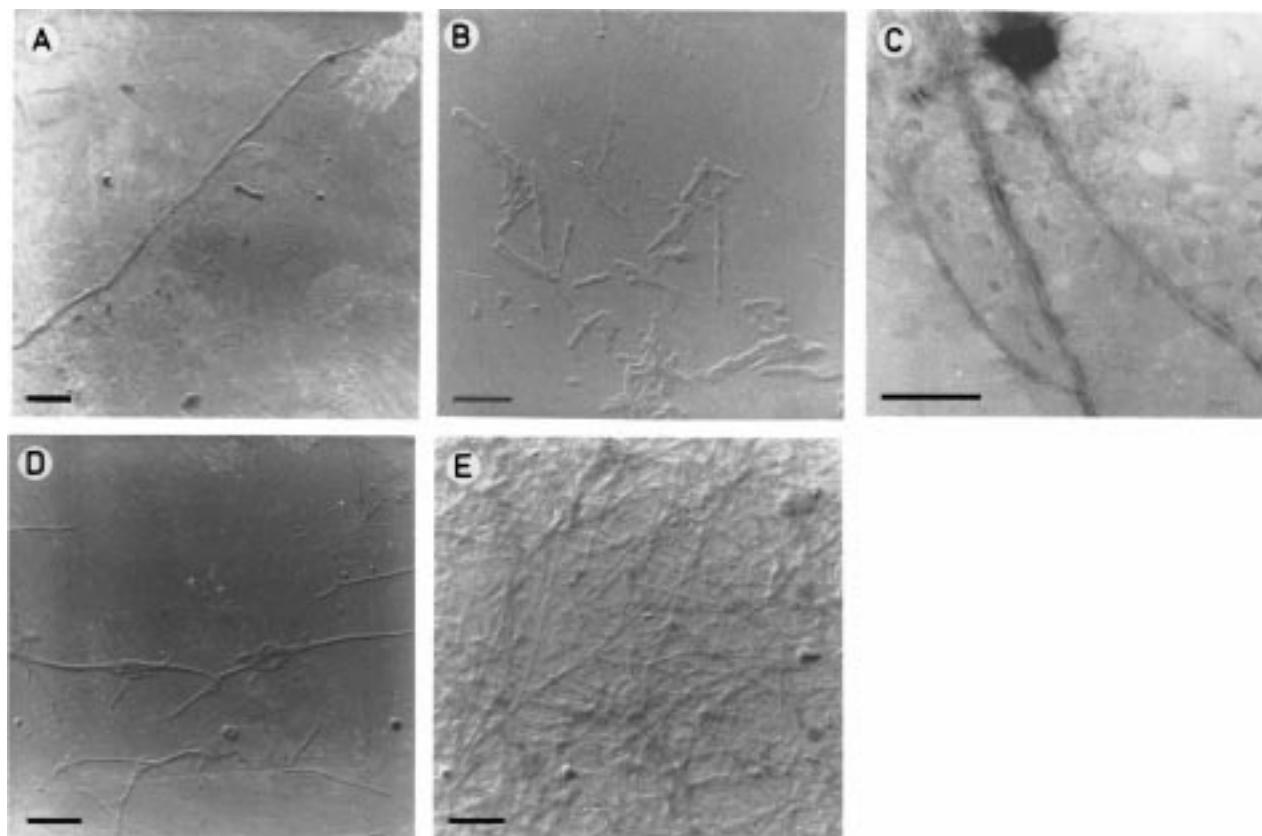


Figure 3. Electron micrographs of Pam₃Cys-Ser derivatives (**2**). Bar represents 500 nm. (A) Pt-Shadowing of freshly prepared dispersion of **2R/S**; (B) Pt shadowing of **2R/S** after aging for 7 days; (C) negative staining of **2R/S** after aging for 7 days; (D) Pt shadowing of freshly prepared dispersion of **2R**; (E) Pt shadowing of **2R** after aging for 7 Days.

Table 2. Molecular Areas and Collapse Pressure of Pam₃Cys Derivatives

compound	molecular area (Å ² /molec.)	collapse pressure (mN/m)
1R/S	56.7	55.0
1R	63.0	56.5
1S	60.9	63.6
2R/S	58.8	40.7
2R	58.5	41.0
2S	57.8	52.1

barrier. This mode of compression should minimize possible viscosity effects on isotherms and explain the marginal changes in the shape of the isotherms and the collapse pressures when the monolayers are compressed more slowly to mimic a thermodynamic mode (1 h/sweep instead of 12 min/sweep). Nevertheless, our measured drop in pressure during the waiting period as well as a smaller compressibility during the second compression in the hysteresis experiment (Figure 4d) and a higher collapse temperature at higher temperature (Figure 4a) supports the notion that the monolayer of **1S/R** is viscous.

The results of the pure diastereoisomers are very interesting. In the hysteresis experiment, a drop in pressure during the first waiting period is observed for **1R** (Figure 4e) but not for **1S** (Figure 4f). Thus, it can be concluded that **1R** is the diastereoisomer responsible for the viscosity of the mixture of diastereoisomers **1S/R**, while pure **1S** forms normal, nonviscous monolayers. The different temperature effects on the isotherms of **1S** and **1R** corroborate this conclusion. Thus, the collapse pressure of **1R** is increased (Figure 4b) like that of **1S/R** (Figure 4a), while the one of **1S** virtually remains the same when the temperature is increased from 20 to 30 °C (Figure 4c). A shoulder in the isotherm between molecular area 60 and 80 Å²/molecule is another unique feature observed for the **1R** epimer

(Figure 4b). This characteristic did not disappear in the hysteresis experiment during the second compression (Figure 4e). It can therefore be concluded that it is not caused by a high viscosity but is due to the coexistence of liquid condensed and liquid expanded phases for **1R**.

It would be of interest to observe this phase separation by microscopy and, in particular, to know if the chirality of the molecules manifests itself in the 2-dimensional crystallites of the liquid condensed phase as they grow during compression of the liquid expanded phase. Such crystallites have been observed by fluorescence microscopy and Brewster angle microscopy in other cases.¹⁵ In the present case, no 2-dimensional crystallization in the coexistence phase was observed by Brewster angle microscopy for any of the studied compounds (**1** and **2 S/R**, **R**, and **S**). Remarkably, the compounds showed a strong tendency to aggregate already in a part of the isotherm where no aggregation was expected, namely, at a pressure of $\pi = 0$ mN/m, which is supposed to represent a “gas-analogous” phase where no interaction between the molecules is expected. As an example, the Brewster angle microscope pictures of the nonviscous (see above) monolayer of **1S** is presented in Figure 5. The first picture shows “floating islands” at $\pi = 0$ mN/m,¹⁶ which became denser and started to fuse upon compression to a surface pressure of 1 mN/m and, eventually, resulted in a mosaic-like monolayer.

(15) (a) Van Esch, J. H.; Nolte, R. J. M.; Ringsdorf, H.; Wildburg, G. *Langmuir* **1994**, *10*, 6, 1955–1961. (b) Sommerdijk, N. A. J. M.; Buynsters, P. J. A. A.; Pistorius, A. M. A.; Wang, M.; Feiters, M. C.; Nolte, R. J. M.; Zwanenburg, B. *J. Chem. Soc., Chem. Commun.* **1994**, *17*, 1941–1942 and correction, 2736. (c) Sommerdijk, N. A. J. M.; Buynsters, P. J. J. A.; Akdemir, H.; Geurts, D. G.; Pistorius, A. M. A.; Feiters, M. C.; Nolte, R. J. M.; Zwanenburg, B. *Chem. Eur. J.* **1998**, *4*, 1, 127–136.

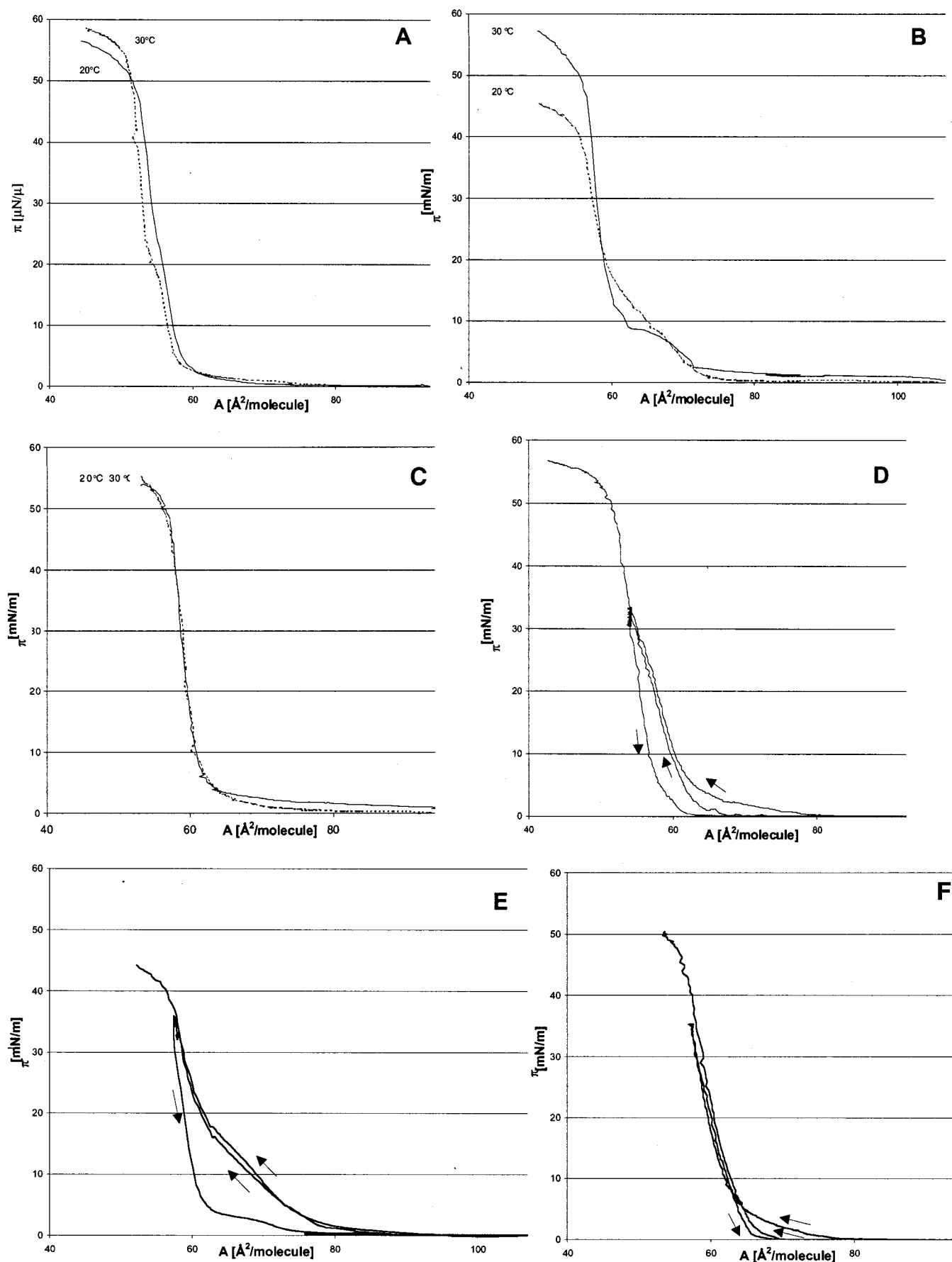


Figure 4. Monolayer properties of Pam₃Cys and Pam₃Cys-Ser derivatives studied by Langmuir-film balance. (A) Temperature dependence of **1R/S**; (B) temperature dependence of **1R**; (C) temperature dependence of **1S**; (D) hysteresis experiment of **1R/S**; (E) hysteresis experiments of **1R**; (F) hysteresis experiments of **1S**.

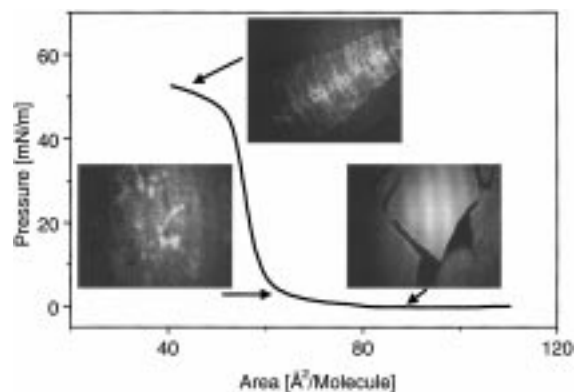


Figure 5. BAM images and isotherm of **1S** (11 °C).

Conclusions

The desirable immunological properties of Pam₃Cys conjugates arise from their intrinsic adjuvant properties such as B-cell, macrophage, and neutrophil activation and the ability to self-assemble to give macromolecular aggregates. Little is known about a possible correlation between self-assembly properties and immunogenicity; however, antigens have to be presented at the surface of macromolecule assemblies to be recognized by the immune system. The first step of the activation cascade involves a nonspecific interaction of the aggregates with plasma membranes of target immunological cells followed by fusion.¹⁷ After fusion, the lipopeptide conjugates arrange in patches or concentrate on one pole at the cell membrane. It has been proposed¹⁸ that the resulting perturbation of the cell membrane may lead to the generation of cell activation signals. Recent studies have also shown that the lipopeptides do not remain at the surface of cells but enter the cell plasma, the nuclear membrane, and even the nucleus within few minutes after incubation of cells with lipopeptides.

It is obvious that the interactions between lipopeptides themselves or with cell membranes must be of great importance for immunological properties. Here, we have demonstrated that the mode of aggregation and the monolayer properties of Pam₃-Cys derivatives are affected by their chirality and additional serine moiety. Correlations have been found between physicochemical properties and biological activities. With respect to the latter, the lipopeptide Pam₃Cys-Ser is a much more potent mitogen than Pam₃Cys. Furthermore, compounds with R stereochemistry in the glyceryl moiety are more active than compounds with the alternative S configuration.

The diastereoisomeric mixture of Pam₃Cys (**1R/S**) formed multilamellar vesicles the morphology of which did not change upon aging. On the other hand, the compounds **1S** and **1R** formed relatively small vesicles, which, after aging, reorganized to mainly rodlike structures. The additional serine moiety impacts self-assembly properties, and the optically pure compounds **2S** and **2R** form highly ordered extended aggregates without the need of aging, whereas the epimeric mixture **2S/R** initially formed vesicles, which upon aging rearranged to extended structures. Thus, biologically more active derivatives, which contain a serine moiety, have a greater predisposition to form thermodynamically more stable tubular or rodlike aggregates. This tendency is even more profound when the samples contain one of the two epimers only.

(16) Van Nostrum, C. F., Ph.D. Thesis, University of Nijmegen, 1995. Kroon, J. M.; Sudholter, E. J. R.; Schenning, A. P. H. J.; Nolte, R. J. M. *Langmuir* **1995**, *11*, 1, 214–220.

(17) Metzger, J. W.; Sawyer, W. H.; Wille, B.; Biesert, L.; Bessler, W. G.; Jung, G. *Biochim. Biophys. Acta* **1993**, *1149*, 1, 29–39.

(18) Jung, G.; Carrera, C.; Brückner, H.; Bessler, W. G. *Liebigs Ann. Chem.* **1983**, *9*, 1608–1622.

Table 3. Concentrations of the Water Suspensions Studied by TEM

	Pt shadowing	negative staining	freeze fracturing	solvent system
1R/S				EtOH/THF (8:2, v/v)
1R	5.2% (w/v)	5.2% (w/v)	16% (w/v)	EtOH/THF (8:2, v/v)
1S	4.6% (w/v)	4.6% (w/v)	-	EtOH/THF (8:2, v/v)
2R/S	5.2% (w/v)	5.2% (w/v)	16.3% (w/v)	EtOH/THF (1:1, v/v)
2R	6.1% (w/v)	6.1% (w/v)	12.9% (w/v)	EtOH/THF (1:1, v/v)
2S	5.4% (w/v)	5.4% (w/v)	21.1% (w/v)	EtOH/THF (1:1, v/v)

All compounds except **1S**, which is the least biologically active of all, form very viscous monolayers. Furthermore, **1R** is the diastereoisomer responsible for the viscosity of the mixture of diastereoisomers **1S/R**. The compounds **2R/S**, **2R**, and **2S**, which all have an additional serine moiety, have very similar molecular areas and isotherms, and thus, the stereochemistry of these compounds has not a detectable impact on their monolayer properties. Monolayer studies in combination with Brewster angle microscopy have shown that Pam₃Cys derivatives have a high tendency to aggregate.

The physicochemical studies described in this report provide a better understanding of a correlation between the configuration and constitution of Pam₃Cys derivatives and biological activity.

Experimental Section

Compounds **1R/S** was synthesized by a known literature procedure^{9a} and gave satisfying NMR, LSIMS, and HRMS data. Compounds **1R**, **1S**, **2R/S**, **2R**, and **2S** were synthesized following a modified literature procedure^{3d} starting from R, S, or racemic glycidol and L-cysteine bis-*t*-butyl ester. Details are provided in Materials and Methods.

Transmission electron microscopy (TEM) was performed on a Philips EM201 instrument using an acceleration voltage of 60 kV. Pt shadowing was performed using an Edwards 306 system. Freeze fracturing experiments were performed in a Balzers freeze etching system BAF 400 D, with samples rapidly frozen in a BAL-TEC JFD 030 jet-freeze device. The π -A-isotherms were recorded on a thermostated Langmuir trough (270 × 70 mm) manufactured by Riegler & Kirsten GmbH (Ultrathin Organic Film Technology). The monolayers were studied during compression with a Brewster angle microscope (NFT BAM-1) equipped with a 10 mW He-NE laser with a beam diameter of 0.68 mm operating at 632.8 nm. The images were detected using a CCD camera and recorded on a Panasonic superVHS video recorder. Monolayers were spread on a thermostated home-built Langmuir trough (140 × 235 mm). Water used for all experiments was purified on a LABCONCO Water Pro PS system.

General Procedure for Pt-Shadowing. The dry compound was dissolved in an appropriate mixture of EtOH and THF. An aliquot of this solution was injected into hot (72 °C) vortexed water. One drop of the resulting homogeneous water suspension was applied to a carbon-coated copper grid. After the aggregates were allowed to settle for one minute, the excess water was drained with filter paper. After drying, the aggregates were shadowed with Pt atoms.

General Procedure for Negative Staining. The water suspension was prepared and applied to a copper grid as described above. Subsequently, a uranyl acetate solution (1:49, v/v) was added for one minute and then removed by filter paper.

General Procedure for Freeze Fracturing and Etching. Aqueous suspensions were prepared as described for Pt shadowing. A freshly cleaned gold (400 mesh) grid was immersed in the suspension and placed between two freshly cleaned copper plates. The grid and copper plates were rapidly frozen in liquid propane and fractured at 10⁻⁶ Torr and -105 °C. After etching (2 min), Pt-shadowing (2 nm), and carbon deposition (20 nm), the resulting replicas were cleaned ~28 h with 70% H₂SO₄ and subsequently transferred to water (several times) and finally dried (Table 3).

Measurement of π -A-Isotherm. Before the measurements were performed, the trough was cleaned with EtOH, which was removed by repeated partial replacement with water. The cleanness of the water surface was confirmed by a surface pressure deviation lower than 0.1 mN/m after compression. Compounds were dissolved in CH₂Cl₂, and

appropriate aliquots of these solutions were spread dropwise on the water surface. After a period of 10 min, the compression was started. The speed of compression was either 1 h/sweep or 12 min/sweep.

Hysteresis Experiments. Hysteresis experiments were carried out as described in the literature.¹³ In brief, the monolayer was compressed to a surface pressure of 35 mN/m, kept at constant area for 5 min, decompressed, kept at constant area for 1 min, and then compressed till it collapsed.

Brewster Angle Microscopy. Monolayers were applied on a water surface as described above. Compression was performed at a speed of 6.89 cm²/min under direct observation of the morphologies by the Brewster angle microscope.

Materials and Methods

¹H and ¹³C NMR spectra were recorded on a Bruker DRX500 (500 and 125 MHz, respectively) and on a Bruker AC300 spectrometer (300 and 75 MHz, respectively). Chemical shifts were measured in ppm from million using the signal of the residual solvent (¹H NMR) or the deuterated solvent (¹³C NMR) as internal standards. LSI and HR mass spectra were recorded using a VG Zabspec mass spectrometer. MALDI TOF mass spectrometry experiments were performed on a Kratos Kompact MALDI III with solutions of *trans*-3-indolacrylic acid (10 mg/mL), *all-trans*-retinoic acid (10 mg/mL) in THF, and gentisic acid (10 mg/mL) in acetonitrile/0.1% aqueous TFA (3:2, v/v) as the matrices and as appropriate. Melting points were measured on a Gallenkamp melting point apparatus and are given uncorrected. Optical rotations were measured on a Perkin-Elmer 457 polarimeter.

Gravity column chromatography was performed on silica gel 60 (Merck, 70-230 mesh). Gel filtration was carried out on a Pharmacia LPLC system (Pharmacia Biotech Gradi Frac System) using Sephadex LH 20 as the stationary phase. Dichloromethane and acetonitrile were purchased from Fishers, distilled from calcium hydride, and stored over 4 Å molecular sieves under argon. *N,N*-Dimethylformamide was purchased from Fishers, distilled from calcium hydride under reduced pressure, and stored over 4 Å molecular sieves under argon. Petroleum ether (60–80 °C) and ethyl acetate were purchased from Fishers as well as dimethyl sulfoxide (GPC grade) for HPLC. Zn powder was activated by treatment with aqueous HCl (32%). 4 Å molecular sieves were purchased from Avocado, activated at 300 °C in *high vacuum*, and stored under nitrogen. FmocSer(O^tBu)-Wang resin was purchased from NovaBiochem, cysteine di-*tert*-butylester from Bachem, piperidine from Fluka, and all other chemicals from Aldrich. Reactions were conducted under anhydrous conditions, under inert gas atmosphere (N₂), and at room temperature if not mentioned otherwise.

***N*-Fluorenylmethoxycarbonyl-S-[2,3-dihydroxy-(2RS)-propyl]-(*R*)-cysteine *tert*-butyl ester (5R/S).** A solution of compound **3** (1.5 g, 1.88 mmol) in DCM (15 mL) was treated with freshly activated Zn powder (862 mg, 13.2 mmol) and a mixture of MeOH/HCl (32%/concentrated H₂SO₄ (100:7:1, v/v/v, 6.5 mL). The reaction mixture was stirred vigorously for 15 min, and subsequently, glycidol (**4R/S**) (1.4 g, 19.4 mmol) was added and the resulting mixture stirred at 40 °C for 5 h. The mixture was concentrated to about half of the original volume and cooled to –4 °C, and KHSO₄ (5%, 2 mL) added. After being stirred at –4 °C for 16 h, the mixture was extracted with DCM (3 × 20 mL), the combined organic layers were washed with water (3 × 15 mL), dried (MgSO₄), and filtered, and the filtrate was concentrated in *vacuo*. Compound **5R/S** (1.78 g) was obtained as a viscous clear oil and used in the next reaction step without further purification.

¹H NMR (CDCl₃, 300 MHz): *two diastereoisomers*, δ 7.74 (d, 4H, Fmoc-Ar., *J*_{CH,CH} = 7.4 Hz, R/S), 7.58 (d, 4H, Fmoc-Ar., *J*_{CH,CH} = 7.4 Hz, R/S), 7.38 (t, 4H, Fmoc-Ar., R/S), 7.29 (t, 4H, Fmoc-Ar., R/S), 5.92–5.72 (m, 2H, NH, R/S), 4.60–4.28 (m, 6H, Cys-CH^α, Fmoc-CH₂, R/S), 4.21 (t, 2H, Fmoc-CH, *J*_{CH,CH₂} = 7.0 Hz, R/S), 3.83–3.65 (m, 2H, S-glyceryl-CH, R/S), 3.65–3.40 (m, 4H, S-glyceryl-OCH₂, R/S), 3.29 (brs, 2H, OH, R/S), 3.03–2.82 (m, 4H, Cys-CH₂, R/S), 2.81–2.00 (m, 6H, S-glyceryl-CH₂, OH, R/S), 1.47 (s, 18H, ^tBu-CH₃, R/S). ¹³C NMR (CDCl₃, 75 MHz): δ 169.9 (Cys-CO), 156.2 (Fmoc-CO), 143.8, 141.3, 127.8, 127.1, 125.2, 120.0 (Fmoc-Ar.), 83.1 (^tBu-C_q), 71.0, 70.9 (S-glyceryl-CH), 67.2 (Fmoc-CH₂), 65.3, 65.1 (S-glyceryl-OCH₂), 54.6 (Cys-CH^α), 47.1 (Fmoc-CH), 36.5, 36.4 (Cys-CH₂), 35.6, 35.5 (S-glyceryl-CH₂), 28.0 (^tBu-CH₃). LSIMS: *m/z* = 496 (M + Na)⁺.

***N*-Fluorenylmethoxycarbonyl-S-[2,3-dihydroxy-(2R)-propyl]-(*R*)-cysteine *tert*-Butyl Ester (5R).** The title compound was prepared according to the procedure described for compound **5R/S** starting from **3** (1.5 g, 1.88 mmol) and R-glycidol (**4R**) (1.4 g, 19.4 mmol). Compound **5R** (1.78 g) was obtained as a clear gum and used in the next reaction step without purification.

¹H NMR (CDCl₃, 300 MHz): δ 7.76 (d, 2H, Fmoc-Ar., *J*_{CH,CH} = 7.4 Hz), 7.61 (d, 2H, Fmoc-Ar., *J*_{CH,CH} = 7.4 Hz), 7.40 (t, 2H, Fmoc-Ar.), 7.31 (t, 2H, Fmoc-Ar.), 5.79 (d, 1H, NH, *J*_{CH,NH} = 7.7 Hz), 4.58–4.46 (m, 1H, Cys-CH^α), 4.39 (d, 2H, Fmoc-CH₂, *J*_{CH,CH₂} = 6.3 Hz), 4.23 (t, 1H, Fmoc-CH), 3.84–3.73 (m, 1H, S-glyceryl-CH), 3.72–3.62 (m, 1H, S-glyceryl-OCH₂a), 3.57–3.45 (m, 1H, S-glyceryl-OCH₂b), 3.17 (brs, 1H, OH), 3.04 (dd, 1H, Cys-CH₂a, *J*_{CH₂a,CH₂b} = 14.2 Hz, *J*_{CH,CH₂} = 4.6 Hz), 2.92 (dd, 1H, Cys-CH₂b, *J*_{CH,CH₂} = 6.1 Hz), 2.81 (dd, 1H, S-glyceryl-CH₂, *J*_{CH₂a,CH₂b} = 13.6 Hz, *J*_{CH,CH₂} = 3.7 Hz), 2.62 (dd, 1H, S-glyceryl-CH₂b, *J*_{CH,CH₂} = 8.6 Hz), 2.09 (brs, 1H, OH), 1.47 (s, 9H, ^tBu-CH₃). ¹³C NMR (CDCl₃, 75 MHz): δ 170.0 (Cys-CO), 156.2 (Fmoc-CO), 143.8, 141.3, 127.8, 127.2, 125.2, 120.1 (Fmoc-Ar.), 83.1 (^tBu-C_q), 71.0 (S-glyceryl-CH), 67.3 (Fmoc-CH₂), 65.1 (S-glyceryl-OCH₂), 54.5 (Cys-CH^α), 47.1 (Fmoc-CH), 36.5 (Cys-CH₂), 35.5 (S-glyceryl-CH₂), 28.0 (^tBu-CH₃). LSIMS: *m/z* = 496 (M + Na)⁺.

***N*-Fluorenylmethoxycarbonyl-S-[2,3-dihydroxy-(2S)-propyl]-(*R*)-cysteine *tert*-Butyl Ester (5S).** The title compound was prepared according to the procedure described for compound **5R/S** starting from **3** (1.5 g, 1.88 mmol) and S-glycidol (**4S**) (1.4 g, 19.4 mmol). Compound **5S** (1.78 g) was obtained as a viscous oil and used in the next reaction step without purification.

¹H NMR (CDCl₃, 300 MHz): δ 7.76 (d, 2H, Fmoc-Ar., *J*_{CH,CH} = 7.4 Hz), 7.60 (d, 2H, Fmoc-Ar., *J*_{CH,CH} = 7.2 Hz), 7.40 (t, 2H, Fmoc-Ar.), 7.32 (t, 2H, Fmoc-Ar.), 5.74 (d, 1H, NH, *J*_{CH,NH} = 7.4 Hz), 4.58–4.45 (m, 1H, Cys-CH^α), 4.41 (d, 2H, Fmoc-CH₂, *J*_{CH,CH₂} = 7.0 Hz), 4.23 (t, 1H, Fmoc-CH), 3.85–3.73 (m, 1H, S-glyceryl-CH), 3.68 (dd, 2H, S-glyceryl-OCH₂a, *J*_{CH₂a,CH₂b} = 11.4 Hz, *J*_{CH,CH₂} = 3.3 Hz), 3.54 (dd, 1H, S-glyceryl-OCH₂b, *J*_{CH,CH₂} = 5.9 Hz), 3.11 (brs, 1H, OH), 3.02 (dd, 1H, Cys-CH₂a, *J*_{CH₂a,CH₂b} = 14.0 Hz, *J*_{CH,CH₂} = 4.8 Hz), 2.93 (dd, 1H, Cys-CH₂b, *J*_{CH,CH₂} = 6.3 Hz), 2.78 (dd, 1H, S-glyceryl-CH₂a, *J*_{CH₂a,CH₂b} = 13.8 Hz, *J*_{CH,CH₂} = 4.2 Hz), 2.65 (dd, 1H, S-glyceryl-CH₂b, *J*_{CH,CH₂} = 7.7 Hz), 2.20 (brs, 1H, OH), 1.49 (s, 9H, ^tBu-CH₃). ¹³C NMR (CDCl₃, 75 MHz): δ 169.7 (Cys-CO), 156.2 (Fmoc-CO), 143.8, 141.3, 127.8, 127.1, 125.2, 120.0 (Fmoc-Ar.), 83.2 (^tBu-C_q), 70.5 (S-glyceryl-CH), 67.3 (Fmoc-CH₂), 65.1 (S-glyceryl-OCH₂), 54.5 (Cys-CH^α), 47.1 (Fmoc-CH), 36.6 (Cys-CH₂), 35.9 (S-glyceryl-CH₂), 28.0 (^tBu-CH₃). LSIMS: *m/z* = 496 (M + Na)⁺.

***N*-Fluorenylmethoxycarbonyl-S-[2,3-bis(palmitoyloxy)-(2RS)-propyl]-(*R*)-cysteine *tert*-Butyl Ester (6R/S).** Palmitic acid (1.74 g, 6.77 mmol), DIPC (1.03 g, 8.16 mmol), and DMAP (105 mg, 0.86 mmol) were added to a solution of compound **5R/S** (1 g, 2.11 mmol) in THF (25 mL). After the mixture was stirred for 2 h, glacial acetic acid (0.9 mL) was added and the mixture was concentrated in *vacuo*. The residue was crystallized from DCM/MeOH (1:20, v/v) at –20 °C to give **6R/S** (1.813 g, 91%) as a white powder: mp 38–42 °C.

¹H NMR (CDCl₃, 300 MHz): *two diastereoisomers*, δ 7.74 (d, 4H, Fmoc-Ar., *J*_{CH,CH} = 7.4 Hz, R/S), 7.59 (d, 4H, Fmoc-Ar., *J*_{CH,CH} = 7.4 Hz, R/S), 7.37 (t, 4H, Fmoc-Ar., R/S), 7.29 (t, 4H, Fmoc-Ar., R/S), 5.69 (d, 1H, NH, *J*_{CH,NH} = 5.0 Hz), 5.66 (d, 1H, NH, *J*_{CH,NH} = 5.5 Hz), 5.20–5.05 (m, 2H, S-glyceryl-CH, R/S), 4.54–4.43 (m, 2H, Cys-CH^α, R/S), 4.39–4.17 (m, 8H, S-glyceryl-OCH₂a, Fmoc-CH₂, Fmoc-CH, R/S), 4.13 (dd, 2H, S-glyceryl-OCH₂b, *J*_{CH₂a,CH₂b} = 5.9 Hz, *J*_{CH,CH₂} = 3.0 Hz, R/S), 4.10 (dd, 2H, S-glyceryl-OCH₂b, *J*_{CH,CH₂} = 2.9 Hz, R/S), 3.07 (dd, 2H, Cys-CH₂a, *J*_{CH₂a,CH₂b} = 13.8 Hz, *J*_{CH,CH₂} = 4.6 Hz, R/S), 2.98 (dd, 2H, Cys-CH₂b, *J*_{CH,CH₂} = 5.1 Hz, R/S), 2.73 (d, 4H, S-glyceryl-CH₂, *J*_{CH,CH₂} = 6.5 Hz, R/S), 2.35–2.19 (m, 8H, Pal-CH₂, R/S), 1.66–1.50 (m, 8H, Pal-CH₂, R/S), 1.46 (s, 18H, ^tBu-CH₃, R/S), 1.22 (brs, 96H, Pal-CH₂, R/S), 0.90–0.80 (m, 12H, Pal-CH₃, R/S). ¹³C NMR (CDCl₃, 75 MHz): δ 143.8, 141.3, 127.7, 127.1, 125.0, 120.0 (Fmoc-Ar.), 70.3 (S-glyceryl-CH), 67.3 (Fmoc-CH₂), 63.5 (S-glyceryl-OCH₂), 54.4 (Cys-CH^α), 47.1 (Fmoc-CH), 35.4 (Cys-CH₂), 34.3, 34.1 (Pal-CH₂), 33.3 (S-glyceryl-CH₂), 31.0, 29.7, 29.5, 29.4, 29.2 (Pal-CH₂), 28.0 (^tBu-CH₃), 24.9, 22.7 (Pal-CH₂), 14.2 (Pal-CH₃). LSIMS: *m/z* = 949 (M + Na)⁺.

***N*-Fluorenylmethoxycarbonyl-S-[2,3-bis(palmitoyloxy)-(2R)-pro-**

pyl]-(**R**)-cysteine *tert*-Butyl Ester (**6R**). The title compound was prepared according to the same procedure as described for compound **6R/S** starting from **5R** (1 g, 2.11 mmol). Compound **6R** (1.99 g, 99%) was obtained as a white powder: mp 45 °C.

¹H NMR (CDCl₃, 300 MHz): δ 7.76 (d, 2H, Fmoc-Ar., *J*_{CH,CH} = 7.7 Hz), 7.70 (d, 2H, Fmoc-Ar., *J*_{CH,CH} = 7.0 Hz), 7.39 (t, 2H, Fmoc-Ar.), 7.31 (t, 2H, Fmoc-Ar.), 5.70 (d, 1H, NH, *J*_{CH,NH} = 5.0 Hz), 5.21–5.09 (m, 1H, S-glyceryl-CH), 4.56–4.45 (m, 1H, Cys-CH^α), 4.41–4.33 (m, 1H, S-glyceryl-OCH₂a), 4.31 (d, 2H, Fmoc-CH₂, *J*_{CH,CH₂} = 3.7 Hz), 4.23 (t, 1H, Fmoc-CH), 4.15 (dd, 1H, S-glyceryl-OCH₂b, *J*_{CH₂a,CH₂b} = 11.8 Hz, *J*_{CH,CH₂} = 5.9 Hz), 3.09 (dd, 1H, Cys-CH₂a, *J*_{CH₂a,CH₂b} = 14.0 Hz, *J*_{CH,CH₂} = 4.4 Hz), 3.00 (dd, 1H, Cys-CH₂b, *J*_{CH,CH₂} = 5.3 Hz), 2.76 (d, 2H, S-glyceryl-CH₂, *J*_{CH,CH₂} = 6.6 Hz), 2.38–2.21 (m, 4H, Pal-CH₂), 1.70–1.60 (m, 4H, Pal-CH₂), 1.48 (s, 9H, ^tBu-CH₃), 1.24 (brs, 48H, Pal-CH₂), 0.87 (t, 6H, Pal-CH₃, *J*_{CH₂,CH₃} = 6.8 Hz). ¹³C NMR (CDCl₃, 75 MHz): δ 173.2, 172.9, 169.4, 155.6 (CO), 143.7, 141.2, 127.6, 127.0, 125.0, 119.9 (Fmoc-Ar.), 82.9 (^tBu-C_q), 70.1 (S-glyceryl-CH), 67.1 (Fmoc-CH₂), 63.4 (S-glyceryl-OCH₂), 54.2 (Cys-CH^α), 47.0 (Fmoc-CH), 35.2 (Cys-CH₂), 34.2, 34.0 (Pal-CH₂), 33.2 (S-glyceryl-CH₂), 31.8, 29.6, 29.4, 29.3, 29.2, 29.0 (Pal-CH₂), 27.9 (^tBu-CH₃), 24.8, 22.6 (Pal-CH₂), 14.0 (Pal-CH₃). LSIMS: *m/z* = 949 (M + Na)⁺.

N-Fluorenylmethoxycarbonyl-*S*-[2,3-bis(palmitoyloxy)-(2S)-propyl]-(**R**)-cysteine *tert*-Butyl Ester (**6S**). The title compound was prepared according to the same procedure as described for compound **6R/S** starting from **5S** (1 g, 2.11 mmol). Compound **6S** (1.762 g, 88%) was obtained as a white powder: mp 41–42 °C.

¹H NMR (CDCl₃, 300 MHz): δ 7.76 (d, 2H, Fmoc-Ar., *J*_{CH,CH} = 7.4 Hz), 7.61 (d, 2H, Fmoc-Ar., *J*_{CH,CH} = 7.0 Hz), 7.39 (t, 2H, Fmoc-Ar.), 7.31 (t, 2H, Fmoc-Ar.), 5.69 (d, 1H, NH, *J*_{CH,NH} = 7.7 Hz), 5.20–5.08 (m, 1H, S-glyceryl-CH), 4.56–4.47 (m, 1H, Cys-CH^α), 4.41–4.32 (m, 1H, S-glyceryl-OCH₂a), 4.31 (d, 2H, Fmoc-CH₂, *J*_{CH,CH₂} = 3.7 Hz), 4.23 (t, 1H, Fmoc-CH), 4.13 (dd, 1H, S-glyceryl-OCH₂b, *J*_{CH₂a,CH₂b} = 11.8 Hz, *J*_{CH,CH₂} = 5.9 Hz), 3.08 (dd, 1H, Cys-CH₂a, *J*_{CH₂a,CH₂b} = 13.4 Hz, *J*_{CH,CH₂} = 4.6 Hz), 3.00 (dd, 1H, Cys-CH₂b, *J*_{CH,CH₂} = 5.1 Hz), 2.76 (d, 2H, S-glyceryl-CH₂, *J*_{CH,CH₂} = 6.3 Hz), 2.28 (t, 4H, Pal-CH₂, *J*_{CH₂,CH₂} = 7.4 Hz), 1.68–1.51 (m, 4H, Pal-CH₂), 1.48 (s, 9H, ^tBu-CH₃), 1.24 (brs, 48H, Pal-CH₂), 0.87 (t, 6H, Pal-CH₃, *J*_{CH₂,CH₃} = 6.1 Hz). ¹³C NMR (CDCl₃, 75 MHz): δ 173.4, 173.0 (CO), 143.8, 141.3, 127.7, 127.1, 125.2, 120.0 (Fmoc-Ar.), 83.1 (^tBu-C_q), 70.3 (S-glyceryl-CH), 67.3 (Fmoc-CH₂), 63.5 (S-glyceryl-OCH₂), 54.4 (Cys-CH^α), 47.1 (Fmoc-CH), 35.4 (Cys-CH₂), 34.3, 34.1 (Pal-CH₂), 33.3 (S-glyceryl-CH₂), 32.0, 29.7, 29.5, 29.4, 29.2 (Pal-CH₂), 28.0 (^tBu-CH₃), 24.9, 22.7 (Pal-CH₂), 14.2 (Pal-CH₃). LSIMS: *m/z* = 949 (M + Na)⁺.

S-[2,3-Bis(palmitoyloxy)-(2R)-propyl]-*N*-palmitoyl-(**R**)-cysteine *tert*-Butyl Ester (**7R**). Compound **6R** (881 mg, 0.93 mmol) was dissolved in DMF/piperidine (10 mL, 1:1, v/v). After being stirred for 2 h, the reaction mixture was concentrated under reduced pressure. The residue was dissolved in DCM/DMF (5:2, v/v, 10 mL), and palmitic acid (420 mg, 1.64 mmol), HONB (294 mg, 1.64 mmol), and DIPC (208 mg, 1.64 mmol) were added. After being stirred for 16 h, the reaction mixture was diluted with DCM (30 mL), filtered, and washed with water (3 × 30 mL), aqueous NaHCO₃ (5%, 3 × 30 mL), and water (3 × 30 mL). The combined aqueous layers were extracted with DCM (3 × 50 mL). The combined organic layers were dried (MgSO₄) and concentrated *in vacuo*. The residue was crystallized from chloroform/MeOH (1:5, v/v, 15 mL) at 0 °C. Compound **7R** (880 mg, 97%) was isolated as a white solid: mp = 56–57 °C.

¹H NMR (CDCl₃, 300 MHz) δ 6.32 (d, 1 H, NH, *J*_{NH,2} = 7.4 Hz), 5.18–5.08 (m, 1H, S-glyceryl-CH), 4.70 (m, 1H, Cys-CH^α), 4.32 (dd, 1H, S-glyceryl-OCH₂a, *J*_{Ha,Hb} = 11.8 Hz, *J*_{Ha,CH} = 3.3 Hz), 4.13 (dd, 1H, S-glyceryl-OCH₂b, *J*_{Hb,CH} = 6.1 Hz), 3.07 (dd, 1H, H-Cys-CH₂a, *J*_{Ha,Hb} = 13.8 Hz, *J*_{Ha,CH} = 4.6 Hz), 2.98 (dd, 1H, Cys-CH₂b, *J*_{3b,2} = 5.1 Hz), 2.73 (d, 2H, S-glyceryl-CH₂a, *J*_{Ha,CH} = 6.6 Hz), 2.30 (m, 4H, 2 Pal-C(O)CH₂), 2.22 (t, 2H, Pal-C(O)CH₂, *J* = 7.7 Hz), 1.70–1.53 (m, 6H, 3 Pal-CH₂), 1.47 (s, 9H, ^tBu-CH₃), 1.37–1.16 (m, 72 H, 3 Pal-CH₂), 0.91–0.82 (m, 9 H, 3 Pal-CH₃); ¹³C NMR (CDCl₃) δ 173.3, 172.9 170.0, (CO), 82.9 (^tBu-C_q), 70.3 (S-glyceryl-OCH), 63.5 (S-glyceryl-OCH₂), 52.5 (Cys-CH^α), 36.5, 35.2, 34.3 34.1, 33.2, 31.9, 29.7,

29.5, 29.4, 29.2 (Cys-CH₂, S-glyceryl-CH₂, Pal-CH₂), 28.0 (^tBu-CH₃), 25.6, 24.9, 22.7 (Pal-CH₂), 14.1 (Pal-CH₃). LSIMS: *m/z* = 989 (100%, [M + Na]⁺).

S-[2,3-Bis(palmitoyloxy)-(2S)-propyl]-*N*-palmitoyl-(**R**)-cysteine *tert*-Butyl Ester (**7S**). The title compound was synthesized following the procedure described for compound **7R**. Compound **6S** (530 mg, 0.56 mmol) was used as a starting material. Compound **7S** (480 mg, 89%) was obtained as a white solid: mp = 62 °C.

¹H NMR (CDCl₃, 300MHz) δ 6.28 (d, 1 H, NH, *J*_{NH,2} = 7.4 Hz), 5.18–5.07 (m, 1H, S-glyceryl-CH), 4.70 (m, 1H, Cys-CH^α), 4.31 (dd, 1H, S-Glyceryl-OCH₂a, *J*_{Ha,Hb} = 12.0 Hz, *J*_{Ha,CH} = 3.5 Hz), 4.12 (dd, 1H, S-Glyceryl-OCH₂b, *J*_{Hb,CH} = 6.1 Hz), 3.02 (d, 2H, Cys-CH₂), 2.72 (m, 2H, H-S-glyceryl-CH₂), 2.35–2.26 (m, 4H, 2 Pal-C(O)CH₂), 2.23 (t, 2H, Pal-C(O)CH₂, *J* = 7.7 Hz), 1.68–1.53 (m, 6H, 3x Pal-CH₂), 1.47 (s, 9H, ^tBu-CH₃), 1.35–1.15 (m, 7 H, 3x Pal-CH₂), 0.91–0.83 (m, 9H, 3x Pal-CH₃). ¹³C NMR (CDCl₃) δ 173.3, 172.9, 169.7 (CO), 82.9 (^tBu-C_q), 70.4 (S-glyceryl-CH), 63.5 (S-glyceryl-OCH₂), 52.4 (Cys-CH^α), 36.5, 35.4, 34.3 34.1, 33.2, 31.9, 29.7, 29.5, 29.4, 29.1 (Cys-CH₂, S-glyceryl-CH₂, Pal-CH₂), 28.0 (^tBu-CH₃), 25.6, 24.9, 22.7 (Pal-CH₂), 14.1 (Pal-CH₃). LSIMS: *m/z* = 989 (100%, [M + Na]⁺).

S-[2,3-Bis(palmitoyloxy)-(2R)-propyl]-*N*-palmitoyl-(**R**)-cysteine (**IR**). Compound **7R** (600 mg, 0.62 mmol) was dissolved in trifluoroacetic acid (6 mL) and stirred for 1 h. The solvent was concentrated *in vacuo*, the residue was treated with water (10 mL), and the waxlike precipitate was washed with cold water (100 mL). Crystallization from chloroform/light petroleum ether (1:16, v/v, 30 mL) afforded compound **IR** (410 mg, 73%) as a white solid: mp = 66 °C.

¹H NMR (CDCl₃) δ 6.58 (d, 1 H, NH, *J*_{NH,CH} = 6.3 Hz), 5.21–5.09 (m, 1H, S-glyceryl-CH), 4.74–4.64 (m, 1H, Cys-CH^α), 4.37–4.28 (m, 1H, S-glyceryl-OCH₂a), 4.10 (dd, 1H, S-glyceryl-OCH₂b, *J*_{Hb,Ha} = 12.0 Hz, *J*_{Hb,CH} = 6.1 Hz), 3.18–2.97 (m, 2H, Cys-CH₂), 2.71 (d, 2H, S-glyceryl-OCH₂, *J*_{CH₂,CH} = 6.3 Hz), 2.35–2.23 (m, 6H, 3x Pal-C(O)-CH₂), 1.68–1.52 (m, 6H, Pal-CH₂), 1.35–1.17 (m, 72H, 3x Pal-CH₂), 0.90–0.82 (m, 9H, 3x Pal-CH₃). ¹³C NMR (CDCl₃) δ 174.5, 173.6, 172.9 (CO), 70.2 (S-glyceryl-CH), 63.8 (S-glyceryl-OCH₂), 52.1 (Cys-CH^α), 36.3, 34.3 34.1, 32.9, 31.9, 29.7, 29.6, 29.4, 29.2 25.6, 24.9, 22.7 (Cys-CH₂, S-glyceryl-CH₂ and Pal-CH₂), 14.1 (Pal-CH₃). LSIMS: *m/z* = 955 (100%, [M + 2Na-H]⁺).

S-[2,3-Bis(palmitoyloxy)-(2S)-propyl]-*N*-palmitoyl-(**R**)-cysteine (**IS**). The title compound was prepared following the procedure described for compound **IR** using **7S** (470 mg, 0.48 mmol) as the starting material. Compound **IS** (370 mg, 84%) was obtained as a white solid: mp = 67–68 °C.

¹H NMR (CDCl₃) δ 6.52 (d, 1 H, NH, *J*_{NH,CH} = 7.0 Hz), 5.20–5.10 (m, 1H, S-glyceryl-CH), 4.77 (m, 1H, Cys-CH^α), 4.37 (dd, 1H, S-glyceryl-OCH₂a, *J*_{Ha,Hb} = 11.8 Hz, *J*_{Ha,CH} = 3.3 Hz), 4.09 (dd, 1H, S-glyceryl-OCH₂b, *J*_{Hb,CH} = 6.4 Hz), 3.10 (d, 2H, Cys-CH₂, *J*_{CH,CH₂} = 5.1 Hz), 2.79–2.64 (m, 2H, S-glyceryl-CH₂), 2.36–2.25 (m, 6H, 3x Pal-C(O)CH₂), 1.69–1.53 (m, 6H, 3x Pal-CH₂), 1.36–1.17 (m, 72 H, 3x Pal-CH₂), 0.91–0.83 (m, 9H, 3x Pal-CH₃). ¹³C NMR (CDCl₃) δ 174.6 173.7, 173.0 (CO), 70.4 (S-glyceryl-CH), 63.9 (S-glyceryl-OCH₂), 52.1 (Cys-CH^α), 36.5, 34.5 34.3, 33.0, 32.0, 29.9, 29.7, 29.5, 29.3, 25.7, 25.1, 22.9 (Cys-CH₂, S-glyceryl-CH₂, Pal-CH₂), 14.3 (Pal-CH₃). LSIMS: *m/z* = 955 (100%, [M + 2Na-H]⁺).

N-Fluorenylmethoxycarbonyl-*S*-[2,3-bis(palmitoyloxy)-(2RS)-propyl]-(**R**)-cysteine (**8R/S**). Compound **6R/S** (1 g, 1.05 mmol) was dissolved in TFA (20 mL), and the mixture was stirred for 1 h and subsequently concentrated *in vacuo*. The oily residue was coevaporated from toluene (3 × 10 mL) and DCM (3 × 10 mL) and finally lyophilized from *tert*-butyl alcohol to afford **8R/S** (917 mg, 99%) as a white solid: mp 64–65 °C.

¹H NMR (CDCl₃, 300 MHz): *two diastereoisomers*, δ 7.76 (d, 4H, Fmoc-Ar., *J*_{CH,CH} = 7.4 Hz, R/S), 7.61 (d, 4H, Fmoc-Ar., *J*_{CH,CH} = 7.0 Hz, R/S), 7.39 (t, 4H, Fmoc-Ar., R/S), 7.31 (t, 4H, Fmoc-Ar., R/S), 5.73 (d, 2H, NH, *J*_{CH,NH} = 7.0 Hz, R/S), 5.26–4.99 (m, 2H, S-glyceryl-CH, R/S), 4.72–4.59 (m, 2H, Cys-CH^α, R/S), 4.45–4.04 (m, 10H, S-glyceryl-OCH₂, Fmoc-CH₂, Fmoc-CH, R/S), 3.23–3.02 (m, 4H, Cys-CH₂, R/S), 2.85–2.60 (m, 4H, S-glyceryl-CH₂, R/S), 2.38–2.19 (m, 8H, Pal-CH₂, R/S), 1.69–1.52 (m, 8H, Pal-CH₂, R/S), 1.25 (brs, 96H, Pal-CH₂, R/S), 0.92–0.83 (m, 12H, Pal-CH₃, R/S). ¹³C NMR (CDCl₃, 75 MHz): δ 174.1, 173.4, 173.3 (CO), 156.9 (Fmoc-CO), 143.6, 141.1,

127.6, 127.0, 125.0, 119.8 (Fmoc-Ar.), 70.1 (S-glyceryl-CH), 67.3 (Fmoc-CH₂), 63.4 (S-glyceryl-OCH₂), not seen (Cys-CH^α), 47.0 (Fmoc-CH), 34.7, 34.2, 34.0, 31.8, 29.4, 29.0 (Cys-CH₂, S-glyceryl-CH₂, Pal-CH₂), 24.8, 22.6 (Pal-CH₂), 14.0 (Pal-CH₃). MALDI TOF MS: *m/z* = 916 ([M + Na]⁺, indolacrylic acid), 915 ([M + Na]⁺, gentisic acid). LSIMS: *m/z* = 938.5 (M + 2Na-H)⁺.

N-Fluorenylmethoxycarbonyl-S-[2,3-bis(palmitoyloxy)-(2R)-propyl]- (R)-cysteine (8R). The title compound was prepared according to a procedure similar to that for compound 8R/S starting from 6R (1 g, 1.05 mmol). Compound 8R (816 mg, 87%) was obtained as a white solid: mp 61 °C.

¹H NMR (CDCl₃, 300 MHz): δ 7.76 (d, 2H, Fmoc-Ar., *J*_{CH,CH} = 7.7 Hz), 7.62 (d, 2H, Fmoc-Ar., *J*_{CH,CH} = 7.0 Hz), 7.39 (t, 2H, Fmoc-Ar.), 7.31 (t, 2H, Fmoc-Ar.), 5.75 (d, 1H, NH, *J*_{CH,NH} = 7.0 Hz), 5.22–5.09 (m, 1H, S-glyceryl-CH), 4.71–4.58 (m, 1H, Cys-CH^α), 4.47–4.05 (m, 5H, S-glyceryl-OCH₂, Fmoc-CH₂, Fmoc-CH), 3.21–3.00 (m, 2H, Cys-CH₂), 2.90–2.60 (m, 2H, S-glyceryl-CH₂), 2.41–2.20 (m, 4H, Pal-CH₂), 1.71–1.52 (m, 4H, Pal-CH₂), 1.24 (brs, 48H, Pal-CH₂), 0.89–0.83 (m, 6H, Pal-CH₃). ¹³C NMR (CDCl₃, 75 MHz): δ 174.4, 173.5, 173.4 (CO), 155.9 (Fmoc-CO), 143.7, 141.3, 127.7, 127.1, 125.1, 120.0 (Fmoc-Ar.), 70.2 (S-glyceryl-CH), 67.4 (Fmoc-CH₂), 63.5 (S-glyceryl-OCH₂), 53.7 (Cys-CH^α), 47.1 (Fmoc-CH), 34.7 (Cys-CH₂), 34.3, 34.1 (Pal-CH₂), 33.0 (S-glyceryl-CH₂), 31.9 (Pal-CH₂), 29.7, 29.5, 29.4, 29.1 (Pal-CH₂), 24.9, 22.7 (Pal-CH₂), 14.1 (Pal-CH₃). LSIMS: *m/z* = 916 (M + Na)⁺.

N-Fluorenylmethoxycarbonyl-S-[2,3-bis(palmitoyloxy)-(2S)-propyl]- (R)-cysteine (8S). The title compound was prepared according to a procedure similar to that described for compound 8R/S starting from 6S (1 g, 1.05 mmol). Compound 8S (924 mg, 99%) was obtained as a white solid: mp 64 °C.

¹H NMR (CDCl₃, 300 MHz): δ 7.75 (d, 2H, Fmoc-Ar., *J*_{CH,CH} = 7.4 Hz), 7.60 (d, 2H, Fmoc-Ar., *J*_{CH,CH} = 7.0 Hz), 7.39 (t, 2H, Fmoc-Ar.), 7.30 (dt, 2H, Fmoc-Ar., *J*_{CH,CH} = 1.1 Hz, *J*_{CH,CH} = 7.4 Hz, *J*_{CH,CH} = 8.5 Hz), 5.74 (d, 1H, NH, *J*_{CH,NH} = 7.7 Hz), 5.22–5.09 (m, 1H, S-glyceryl-CH), 4.72–4.60 (m, 1H, Cys-CH^α), 4.46–4.28 (m, 3H, S-glyceryl-OCH₂a, Fmoc-CH₂), 4.24 (t, 1H, Fmoc-CH, *J*_{CH,CH₂} = 7.0 Hz), 4.02 (dd, 1H, S-glyceryl-OCH₂b, *J*_{CH₂a,CH₂b} = 12.1 Hz, *J*_{CH,CH₂} = 6.1 Hz), 3.21–3.00 (m, 2H, Cys-CH₂), 2.90–2.60 (m, 2H, S-glyceryl-CH₂), 2.40–2.20 (m, 4H, Pal-CH₂), 1.71–1.52 (m, 4H, Pal-CH₂), 1.25 (brs, 48H, Pal-CH₂), 0.92–0.81 (m, 6H, Pal-CH₃). ¹³C NMR (CDCl₃, 75 MHz): δ 174.3, 173.6, 1.73.3 (CO), 155.8 (Fmoc-CO), 143.7, 141.3, 127.8, 127.1, 125.6, 120.0 (Fmoc-Ar.), 70.3 (S-glyceryl-CH), 67.4 (Fmoc-CH₂), 63.6 (S-glyceryl-OCH₂), 53.6 (Cys-CH^α), 47.1 (Fmoc-CH), 34.6 (Cys-CH₂), 34.3, 34.1 (Pal-CH₂), 29.7, 29.4, 29.2 (Pal-CH₂), 23.2, 22.7 (Pal-CH₂), 14.2 (Pal-CH₃). LSIMS: *m/z* = 939 (M + 2Na-H)⁺.

N-Palmitoyl-S-[2,3-bis(palmitoyloxy)-(2RS)-propyl]- (R)-cysteinylnyl-(S)-serine (2R/S). Wang resin containing *N*-Fmoc-*O*-(*tert*-butyl)-serine (9) (200 mg, loading 0.82 mmol/g) was pre-swollen in DMF and the Fmoc group cleaved by treatment with piperidine/DMF (2:8, v/v, 10 mL, 30 min) as indicated by a positive Kaiser test. The solvent was removed and the resin washed with DMF (30 mL, 4 × 10 min). The mixture was suspended in DCM/DMF (5:2, v/v, 14 mL), 8R/S (293 mg, 0.328 mmol), HONB (59 mg, 0.328 mmol), and DIPC (42 mg, 0.328 mmol) were added, the mixture was agitated for 5 h when a negative Kaiser test indicated completion of the coupling reaction. The solvent was removed and the resin washed with DCM/DMF (5:2, v/v, 28 mL, 3 × 10 min) and subsequently treated with piperidine/DMF (2:8, v/v, 10 mL, 30 min). A positive Kaiser test indicated cleavage of the Fmoc group. The solvent was removed, the resin was washed with DMF (30 mL, 4 × 10 min) and subsequently suspended in DCM/pyridine (1:1, v/v, 10 mL), and palmitoyl chloride (451 mg, 1.64 mmol) was added. After agitation for 3 h, a negative Kaiser test indicated a complete coupling reaction. The solvent was removed and the resin washed with DCM/DMF (5:2, v/v, 28 mL, 3 × 10 min) and DCM (28 mL, 3 × 10 min). The dry resin was treated with TFA/water (95:5, v/v, 10 mL) for 1 h. The solvent was removed by filtration and the resin washed with TFA (2 × 5 mL). The combined filtrates were concentrated in vacuo and lyophilized from *tert*-butyl alcohol. The white residue was purified by gel filtration (Sephadex LH-20, MeOH/DCM, 1:1, v/v) to afford 2R/S (127.5 mg, 78%) as a colorless sticky foam.

¹H NMR (CDCl₃, 500 MHz): two diastereoisomers, δ 7.64 (brs, 2H, Ser-NH, R/S), 6.83 (brs, 2H, Cys-NH, R/S), 5.23 (brs, 2H, Ser-OH, R/S), 5.17 (brs, 2H, S-glyceryl-CH, R/S), 4.70 (brs, 2H, Cys-CH^α, R/S), 4.57 (brs, 2H, Ser-CH^α, R/S), 4.35 (dd, 2H, S-glyceryl-OCH₂a, *J*_{CH₂a,CH₂b} = 18.1 Hz, *J*_{CH,CH₂} = 11.6 Hz, R/S), 4.20–4.09 (m, 2H, S-glyceryl-OCH₂b, R/S), 4.04 (brs, 2H, Ser-OCH₂a, R/S), 3.89 (brs, 2H, Ser-OCH₂b, R/S), 3.18–2.87 (m, 4H, Cys-CH₂, R/S), 2.82–2.68 (m, 4H, S-glyceryl-CH₂, R/S), 2.36–2.20 (m, 12H, Pal-CH₂, R/S), 1.69–1.54 (m, 12H, Pal-CH₂, R/S), 1.25 (brs, 144H, Pal-CH₂, R/S), 0.88 (t, 18H, Pal-CH₃, *J*_{CH₂,CH₃} = 7.0 Hz, R/S). ¹³C NMR (CDCl₃, 125 MHz): δ 174.6, 174.5, 173.8, 173.6, 173.6, 170.6 (CO), 70.3 (S-glyceryl-CH), 63.8, 63.8 (S-glyceryl-OCH₂), 62.6 (Ser-OCH₂), 55.2 (Ser-CH^α), 52.6, 52.2 (Cys-CH^α), 36.4, 34.5, 34.4, 34.1 (Pal-CH₂), 32.8, 32.4 (S-glyceryl-CH₂), 31.9, 29.7, 29.6, 29.3, 29.2, 25.6, 24.9, 24.9, 22.7 (Pal-CH₂), 14.1 (Pal-CH₃). LSIMS: *m/z* = 1019.9 (M + Na)⁺.

N-Palmitoyl-S-[2,3-bis(palmitoyloxy)-(2R)-propyl]- (R)-cysteinylnyl-(S)-serine (2R). The title compound was prepared according to a procedure similar to that described for compound 2R/S starting from Wang resin containing *N*-Fmoc-*O*-(*tert*-butyl)-serine (9) (200 mg, loading 0.82 mmol/g) and 8R (293 mg, 0.328 mmol). After purification by gel filtration chromatography (Sephadex LH-20, MeOH/DCM, 1:1, v/v), 2R (100 mg, 61%) was obtained as a white powder. [α]_D²⁵ = –10.0° (DCM, *c* = 11.28 mg/mL): mp 67–69 °C.

¹H NMR (CDCl₃, 500 MHz): δ 7.55 (brs, 1H, Ser-NH), 6.71 (d, 1H, Cys-NH, *J*_{CH,NH} = 6.2 Hz), 5.17–5.05 (m, 1H, S-glyceryl-CH), 4.72–4.59 (m, 1H, Cys-CH^α), 4.53 (brs, 1H, Ser-CH^α), 4.26 (dd, 1H, S-glyceryl-OCH₂a, *J*_{CH₂a,CH₂b} = 11.8 Hz, *J*_{CH,CH₂} = 2.5 Hz), 4.08 (dd, 1H, S-glyceryl-OCH₂b, *J*_{CH,CH₂} = 6.3 Hz), 3.99 (d, 1H, Ser-CH₂a, *J*_{CH₂a,CH₂b} = 7.0 Hz), 2.92 (dd, 1H, Cys-CH₂a, *J*_{CH₂a,CH₂b} = 13.6 Hz, *J*_{CH,CH₂} = 5.0 Hz), 2.84 (dd, 1H, Cys-CH₂a, *J*_{CH,CH₂} = 6.8 Hz), 2.76–2.62 (m, 2H, S-glyceryl-CH₂), 2.30–2.13 (m, 6H, Pal-CH₂), 1.59–1.49 (m, 6H, Pal-CH₂), 1.19 (brs, 79H, Pal-CH₂, OH), 0.84–0.77 (m, 9H, Pal-CH₃). ¹³C NMR (CDCl₃, 125 MHz): δ 174.6, 173.9, 173.6, 170.5 (CO), 70.3 (S-glyceryl-CH), 63.8 (S-glyceryl-OCH₂), 62.6 (Ser-OCH₂), 55.0 (Ser-CH^α), 52.5 (Cys-CH^α), 36.4 (Pal-CH₂), 34.6 (Cys-CH₂), 34.4, 34.1 (Pal-CH₂), 32.8 (S-glyceryl-CH₂), 31.9, 29.7, 29.6, 29.4, 29.2, 25.6, 25.0, 24.9, 22.7 (Pal-CH₂), 14.1 (Pal-CH₃). LSIMS: *m/z* = 1019.8 (M + Na)⁺. HRMS (LSIMS): calcd for C₅₇H₁₀₈N₂O₉-SNa (M + Na)⁺ 1019.7673, found 1019.7674.

N-Palmitoyl-S-[2,3-bis(palmitoyloxy)-(2S)-propyl]- (R)-cysteinylnyl-(S)-serine (2S). The title compound was prepared according to the same procedure as described for compound 2R/S starting from Wang resin containing *N*-Fmoc-*O*-(*tert*-butyl)-serine (200 mg, loading 0.82 mmol/g) and 8S (293 mg, 0.328 mmol). After purification by gel filtration column chromatography (Sephadex LH-20, MeOH/DCM, 1:1, v/v), 2S (148.8 mg, 91%) was obtained as a white powder. [α]_D^{22.5} = –22.8° (DCM, *c* = 2.67 mg/mL): mp 69–70 °C.

¹H NMR (CDCl₃, 500 MHz): δ 7.66 (d, 1H, Ser-NH, *J*_{CH,NH} = 6.8 Hz), 6.79 (d, 1H, Cys-NH, *J*_{CH,NH} = 7.5 Hz), 5.22 (brs, 1H, Ser-OH), 5.21–5.11 (m, 1H, S-glyceryl-CH), 4.77–4.66 (m, 1H, Cys-CH^α), 4.59 (brs, 1H, Ser-CH^α), 4.37 (dd, 1H, S-glyceryl-OCH₂a, *J*_{CH₂a,CH₂b} = 12.0 Hz, *J*_{CH,CH₂} = 2.8 Hz), 4.14 (dd, 1H, S-glyceryl-OCH₂b, *J*_{CH,CH₂} = 6.3 Hz), 4.06 (d, 1H, Ser-OCH₂a, *J*_{CH,CH₂} = 10.1 Hz), 3.91 (d, 1H, Ser-OCH₂b, *J*_{CH,CH₂} = *J*_{CH₂a,CH₂b} = 10.0 Hz), 2.98 (dd, 1H, Cys-CH₂a, *J*_{CH₂a,CH₂b} = 13.9 Hz, *J*_{CH,CH₂} = 5.5 Hz), 2.92 (dd, 1H, Cys-CH₂b, *J*_{CH,CH₂} = 7.0 Hz), 2.78 (dd, 1H, S-glyceryl-CH₂a, *J*_{CH₂a,CH₂b} = 14.1 Hz, *J*_{CH,CH₂} = 6.2 Hz), 2.73 (dd, 1H, S-glyceryl-CH₂b, *J*_{CH,CH₂} = 6.4 Hz), 2.36–2.20 (m, 6H, Pal-CH₂), 1.66–1.54 (m, 6H, Pal-CH₂), 1.25 (brs, 72H, Pal-CH₂), 0.91–0.85 (m, 9H, Pal-CH₃). ¹³C NMR (CDCl₃, 125 MHz): δ 174.5, 173.7, 172.7, 172.5, 170.6 (CO), 70.3 (S-glyceryl-CH), 63.8 (S-glyceryl-OCH₂), 62.6 (Ser-OCH₂), 55.0 (Ser-CH^α), 52.2 (Cys-CH^α), 36.4, 34.5, 34.4, 34.1 (Pal-CH₂), 32.3 (S-glyceryl-CH₂), 31.9, 31.7, 29.7, 29.6, 29.4, 29.2, 29.0, 25.6, 24.9, 24.9, 22.7 (Pal-CH₂), 14.1 (Pal-CH₃). LSIMS: *m/z* = 1019.8 (M + Na)⁺. HRMS (LSIMS): calcd for C₅₇H₁₀₈N₂O₉SNa (M + Na)⁺ 1019.7673, found 1019.7672.